

A Domain Wall Model for SMA Characterization

Jordan E. Massad¹ and Ralph C. Smith²

Center for Research in Scientific Computation, N.C. State Univ., Raleigh, NC 27695

ABSTRACT

We develop a model that quantifies constitutive nonlinearities and hysteresis inherent to ferroelastic compounds, with emphasis placed on shape memory alloys. We formulate the model in two steps. First, we use the Landau theory of phase transitions to characterize the effective Gibbs free energy for both single-crystal and polycrystalline ferroelastics. The resulting nonlinear equations model ideal material behavior in the absence of impurities. Second, we incorporate pinning losses to account for the energy required to move domain walls across material inclusions. We illustrate aspects of the model through comparison with experimental stress-strain data.

Keywords: Shape memory alloy, ferroelastic domain, pseudoelasticity, domain wall model, Landau theory of phase transitions

1. INTRODUCTION

Shape memory alloys (SMAs) are being considered for a number of current high performance applications due to their capability to achieve very high work densities, produce large deformations, and generate high stresses if constrained during shape recovery. Furthermore, with the one-way and two-way shape memory effects intrinsic to the material, SMA actuators offer a reduction of mass and of mechanical complexity, in comparison to other actuators. SMA are presently being considered as actuators for applications such as deformable aircraft wings, and adaptive earthquake-proof structures [1, 21]. More recently, microelectromechanical systems (MEMS) devices have used SMAs in actuators, such as micropumps and microgrippers, that are smaller than and exceed the output of their electromagnetic counterparts [6, 29].

In general, the material behavior of SMAs is nonlinear and hysteretic, so it is a nontrivial task to control precisely the motion of SMAs in actuators. To achieve the full potential of SMA actuators, it is necessary to develop models that characterize the nonlinearities and hysteresis inherent in the constituent materials. In conjunction, the design of SMA actuators necessitates the development of control algorithms based on those models. In the last 20 years, there have been a number of advances in SMA modelling and we refer the reader to [4, 10, 12] for reviews of SMA models. Two main types of SMA models are *micromechanical models* and *macroscopic models*. Micromechanical models, such as the one in [18], focus on quantifying how microscopic structural dynamics effect macroscopic behavior. In general, micromechanical models are complex, involve many parameters, and are not intended for model-based control methods. *Macroscopic models* such as those in [7, 9, 13, 14] focus on observed behavior of bulk specimens. Most of these models are phenomenological and they usually resolve the micromechanical behavior to obtain effective or “mesoscopic” descriptions. These models are suitable for implementation into model-based control methods and into finite element methods.

Our objective is to develop a simple model that can simulate nonlinear behavior of SMAs and that admits a low-order formulation suitable for subsequent control design. Analogous to the domain wall models of Jiles and

¹Email: jmassad@unity.ncsu.edu; Telephone: 919-515-3745

²Email: rsmith@unity.ncsu.edu; Telephone: 919-515-7552

Atherton for *ferromagnetics* [15] and of Smith and Hom for *ferroelectrics* [22], we derive a domain wall model for *ferroelastics*, particularly SMAs. We develop the model in two steps. In the first, we formulate the elastic energy stored in a polycrystalline ferroelastic. We achieve this by first considering the elastic energy for a single crystal and then by employing averaging techniques to obtain an effective energy for a polycrystal. The resulting nonlinear constitutive equations predict hysteresis in which phase transformations occur instantaneously and phase boundaries propagate unhindered. In the second step, we incorporate the effects of material inclusions and formulate the energy dissipated by the motion of phase boundaries across those inclusions. The resulting domain wall model predicts stress-strain hysteresis under quasi-static, isothermal conditions. We illustrate the performance of our model through a fit to stress-strain data of a NiTi wire.

We end this section with a basic description of SMA behavior pertinent to our model. In Sections 2 and 3, we develop nonlinear constitutive relations that characterize the stress-strain behavior of ferroelastic compounds. In Section 4, we validate our model with experimental SMA data.

1.1. Shape Memory Alloys

Shape memory alloys recover from up to 10% deformations via stress and temperature-induced phase transformations. The phase transformations occur between two solid phases, called *Martensite* and *Austenite*, each distinguished by a different crystallographic configuration. SMAs recover or “remember” shape by two different mechanisms. First, the *shape memory effect* describes the phenomenon where the original shape of a plastically deformed sample is restored by heating. Upon heating deformed Martensite, it transforms into Austenite and the SMA recovers its shape. Second, SMAs exhibit *pseudoelasticity* at temperatures where Austenite is a stable phase. In this case, Austenite transforms into Martensite due to an applied load. Upon unloading, the material reverts to Austenite and the SMA returns to its original geometry.

For this paper, we model SMAs in isothermal conditions, so we concentrate on pseudoelasticity. Refer to [11] for details of the shape memory effect and other SMA mechanisms. In general, there are 24 crystallographically-similar versions of a Martensite crystal and there is only one version of Austenite. If we confine crystal motions to one axis, a single crystal of SMA admits either the Austenite (A) phase or one of two Martensite variants (M^\pm). As illustrated in Figure 1, M^\pm are sheared versions of A . In the pseudoelastic regime, applying a stress to an SMA crystal induces a transformation to Martensite. As illustrated in Figure 2, experiments show there is a hysteresis associated with these stress-induced phase transitions. Upon loading in the Austenite phase, a specimen behaves elastically until a loading transition point is reached. Loading beyond this point produces a transformation to the Martensite phase. Upon unloading in the Martensite phase, the crystal transforms back

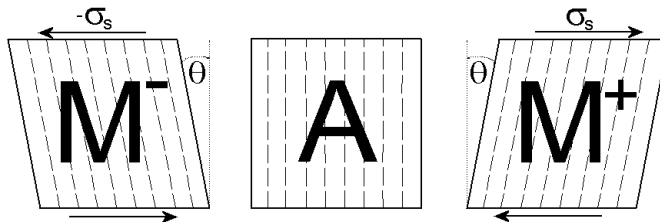


Figure 1. An SMA crystal under 1-D shear loading σ_s admits three configurations (phases): Austenite (A) and Martensite variants (M^\pm). By definition, the shear strain $\varepsilon_s = \tan\theta$.

to Austenite exhibiting zero strain (shape recovery). Thus, the stress-strain behavior of SMAs is nonlinear. We derive nonlinear stress-strain equations in Section 2.3 to model this behavior.

A *single-crystal* SMA refers to a homogeneous, isotropic SMA specimen that consists of unit cells of only one crystallographic orientation. A *polycrystalline* SMA consists of many single-crystal domains with different orientations. SMAs can be prepared as a single crystal, but they occur more naturally as polycrystalline compounds. The behavior of single-crystal SMAs differs from that of polycrystalline SMAs in several aspects. For instance, single-crystal NiTi recovers from 3-10% tensile strains, depending on the crystal orientation, while polycrystalline NiTi typically recover 4-8% tensile strains [3]. We model both single-crystal and polycrystalline SMAs.

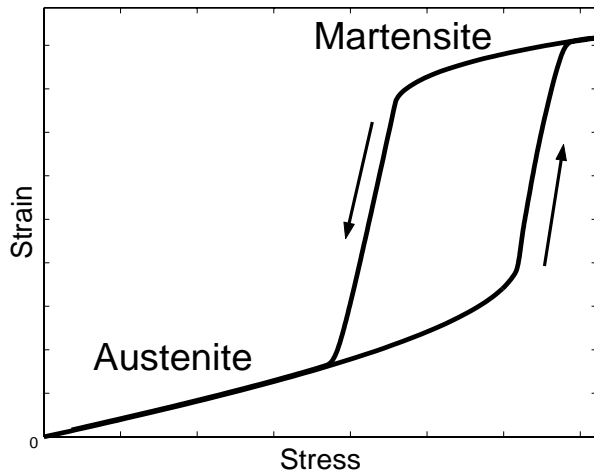


Figure 2: Observed pseudoelastic response of SMAs under uniaxial loading.

2. FREE ENERGY RELATIONS

In this section, we derive the free energy relations for the pseudoelastic behavior of shape memory alloys. First, we use Landau’s theory of phase transitions to quantify the free energy of a single SMA crystal as a function of strain. In particular, we are interested in the *Gibbs free energy* function, which we use to describe the energy of an SMA when we apply a fixed stress at a constant temperature. We refer the reader to [5, 20, 25] for detailed treatments of thermodynamic principles pertinent to this discussion.

Second, we adapt the energy function for a single-crystal element, to accommodate bulk polycrystalline specimens under tensile loading. Third, we obtain stress-strain equations from the polycrystal energy expression, and we conclude by incorporating effects of nonuniform stress fields. Our ultimate result is an equilibrium relation predicting relative elongation due to an applied stress at a fixed temperature for both single-crystal and polycrystalline ferroelastic materials.

2.1. The Landau Potential

To quantify the Gibbs free energy of an SMA crystal, we employ the Landau theory of phase transitions. For a detailed description of the theory, refer to [27]. Others, notably F. Falk, have applied the theory for the

characterization of SMAs [7, 9, 5, 20, 23, 2]. Applying the Landau theory to a physical system, such as an SMA, involves two main steps. The first involves the identification of a quantity of the system that distinguishes one phase from another. This characteristic quantity is called the *order parameter*. In the second, one constructs an expression for the system’s free energy density (per unit volume) as a function of the order parameter. The phenomenological expression for the free energy density is termed the *Landau potential*.

In the case of SMAs, high-temperature Austenite differs from low-temperature Martensite by a shear deformation. Accordingly, Falk derives the SMA order parameter from a second-order strain tensor that corresponds to the three-dimensional deformation of Austenite into Martensite [9]. In our one-dimensional model, an SMA crystal deforms along only one axis. Therefore, the order parameter for our model is the scalar shear strain, $\varepsilon_s = \tan \theta$, where θ is depicted in Figure 1.

For a scalar order parameter ε_s , Tolédano [27] shows that the free energy function has a power series representation of the form

$$L(\varepsilon_s; \sigma_s, T) = \sum_{j=0}^{\infty} F_j(\sigma_s, T) \varepsilon_s^j, \quad (1)$$

where L is the Landau potential and coefficients $F_j(\sigma_s, T)$ are analytic functions of the system temperature T and the shear stress, σ_s . Typically, one chooses the coefficients $F_j(\sigma_s, T)$ by empirical considerations. In addition, one truncates the power series to obtain an explicit function that can approximate experimental data reasonably. Falk determined that the *simplest* Landau potential that characterizes SMAs in one dimension is

$$L_6(\varepsilon_s; \sigma_s, T) = \frac{a_6}{6} \varepsilon_s^6 - \frac{a_4}{4} \varepsilon_s^4 + \frac{a_2}{2} (T - T_c) \varepsilon_s^2 - \sigma_s \varepsilon_s \quad (2)$$

where the coefficients a_2 , a_4 and a_6 are positive constants and the temperature $T_c > 0$ is the transition temperature below which Austenite does not exist [7]. The term $\sigma_s \varepsilon_s$ represents the work done by an external stress. Falk’s Landau potential has up to three minima; the energy minimum at $\varepsilon_s = 0$ corresponds to the Austenite phase, while the symmetric lateral minima correspond to the Martensite variants as illustrated in Figure 3.

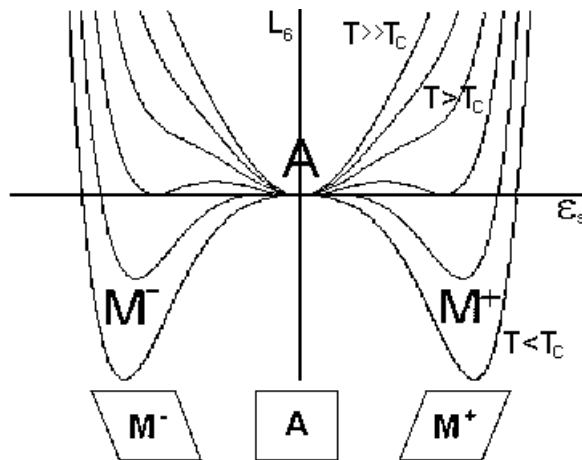


Figure 3. Falk’s Landau potential for low (bottom) to high (top) temperatures at zero stress [7]. For $T < T_c$, only the Martensite variants exist. For high temperatures $T \gg T_c$, only Austenite exists.

For our model, we consider a general extension to (2)

$$L_m(\varepsilon_s; \sigma_s, T) = \sum_{j=3}^m \left(\frac{a_{2j}}{2j} \right) \varepsilon_s^{2j} - \frac{a_4}{4} \varepsilon_s^4 + \frac{a_2}{2} (T - T_c) \varepsilon_s^2 - \sigma_s \varepsilon_s,$$

where a_{2j} ($j = 1, 2, \dots, m$) are constants with $a_2, a_4 > 0$. We also require that $a_{2m} > 0$ so that large deformations correspond to positive free energies. Furthermore, in [27] Tolédano concludes that m must be odd to accommodate SMA behavior. Finally, we obtain an explicit expression for the Gibbs free energy density of an SMA crystal

$$G(\varepsilon_s; \sigma_s, T) = \sum_{j=3}^m \left(\frac{a_{2j}}{2j} \right) \varepsilon_s^{2j} - \frac{a_4}{4} \varepsilon_s^4 + \frac{a_2}{2} (T - T_c) \varepsilon_s^2 - \sigma_s \varepsilon_s, \quad (3)$$

where a_{2j} ($j = 1, 2, \dots, m$) are constants with $a_2, a_4, a_{2m} > 0$, and $m \geq 3$ is odd.

2.2. Macroscopic Description

In practice, the shear force exerted on a single crystal is the result of a tensile force applied to the macroscopic specimen. As shown in [17],

$$\sigma_s = \sigma \sin \phi \cos \phi \quad (4)$$

$$\varepsilon = \varepsilon_s \sin \phi \cos \phi, \quad (5)$$

where the crystal is oriented at an angle ϕ with respect to the applied stress σ , and the measured relative elongation of the specimen is ε . Therefore, (3) can be formulated as

$$G_\phi(\varepsilon; T, \sigma) = \sum_{j=3}^m \left(\frac{\bar{a}_{2j}(\phi)}{2j} \right) \varepsilon^{2j} - \frac{\bar{a}_4(\phi)}{4} \varepsilon^4 + \frac{\bar{a}_2(\phi)}{2} (T - T_c) \varepsilon^2 - \sigma \varepsilon, \quad (6)$$

where

$$\bar{a}_{2j}(\phi) = a_{2j} \left(\frac{2}{\sin(2\phi)} \right)^{2j}, \quad \phi \in \left(0, \frac{\pi}{2} \right), \quad (7)$$

for $j = 1, 2, \dots, m$. Note that for a given ϕ , (6) has the same form as (3).

Ultimately, as detailed in [16] and as suggested by Falk in [7], the effective Gibbs free energy density corresponding to a *polycrystal* is derived from (6) and has the same form as (3), where the coefficients reflect average values over a distribution of polycrystal grain orientations. Therefore, we treat (3) as the form of the Gibbs free energy function with macroscopic quantities σ and ε for both single-crystal and polycrystalline SMAs.

2.3. Stress-Strain Equations

We now derive a stress-strain law from (3) by employing equilibrium thermodynamics. Given a temperature T and a stress σ , the state of equilibrium of the SMA is the value ε that yields a minimum Gibbs free energy. The values of ε that are equilibrium states distinguish the different phases of the SMA. The stable equilibrium states (ε, T, σ) must satisfy the stable equilibrium conditions

$$\left. \frac{\partial G}{\partial \varepsilon} \right|_{\sigma, T} = 0 \quad \text{and} \quad \left. \frac{\partial^2 G}{\partial \varepsilon^2} \right|_{\sigma, T} > 0. \quad (8)$$

Thus, we obtain the stress-strain equation for single-crystal and polycrystalline SMAs

$$\sum_{j=3}^m a_{2j} \varepsilon(\sigma)^{2j-1} - a_4 \varepsilon(\sigma)^3 + a_2 (T - T_c) \varepsilon(\sigma) = \sigma \quad (9)$$

subject to

$$\sum_{j=3}^m (2j - 1) a_{2j} \varepsilon(\sigma)^{2j-2} - 3a_4 \varepsilon(\sigma)^2 + a_2 (T - T_c) > 0. \quad (10)$$

Given a stress σ at temperature T , $\varepsilon(\sigma)$ is the resulting strain that satisfies (9). The coefficients a_{2j} ($j = 1, 2, \dots, m$) of (3) are specimen-dependent and they coincide with high-order elastic constants [26]. In general, we determine the effective coefficients in (9) for a specific SMA or transducer through a least-squares fit to data.

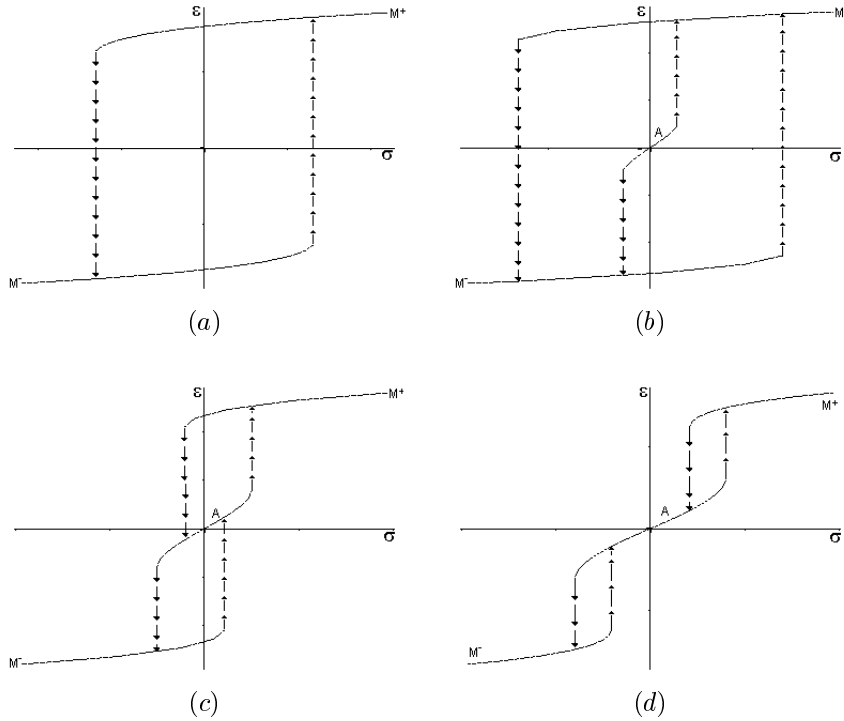


Figure 4. Stress-strain hysteresis predicted by (9) ($m=3$) for increasing temperatures, from $T < T_c$ (a) to the pseudoelastic regime (d).

The stress-strain relationship (9) is nonlinear and multivalued. As shown in Figure 4, it predicts a temperature-dependent stress-strain hysteresis. Note that the model predicts instantaneous phase transitions, corresponding to the discontinuities in the hysteresis loops. This behavior is a characteristic of the Landau theory of phase transitions, since we implicitly assume that a crystal can reach equilibrium instantaneously. In Section 3, we incorporate phase boundary effects which eliminate the discontinuous transitions.

2.4. Nonuniform Stress Effects

In polycrystalline SMAs, cells of single-crystals are randomly oriented. This structure yields a nonuniform stress field in the specimen. To include the effects of the nonuniform stress field, we use a *mean-field* approach

analogous to that used in [15, 22]. We represent the total loading experienced by a crystal element as the effective stress σ_e , which includes both the stress applied to the SMA and an internal stress field contribution

$$\sigma_e = \sigma - \alpha\varepsilon, \quad (11)$$

where $\alpha \geq 0$ is a mean-field constant and ε is the average strain exhibited by the SMA, as modeled in (9). The mean-field constant represents the average stress field variation over the SMA volume. In particular, the case $\alpha = 0$ corresponds to a homogeneous single-crystal SMA where there are no field variations throughout the uniform crystal lattice. Finally, we obtain the complete constitutive stress-strain law for SMAs, which incorporates nonuniform internal stresses

$$\begin{aligned} & \sum_{j=3}^m a_{2j} \varepsilon(\sigma)^{2j-1} - a_4 \varepsilon(\sigma)^3 + a_2 (T - T_c) \varepsilon(\sigma) = \sigma_e \\ \Rightarrow & \sum_{j=3}^m a_{2j} \varepsilon(\sigma)^{2j-1} - a_4 \varepsilon(\sigma)^3 + (a_2 (T - T_c) + \alpha) \varepsilon(\sigma) = \sigma, \end{aligned} \quad (12)$$

subject to

$$\sum_{j=3}^m (2j - 1) a_{2j} \varepsilon(\sigma)^{2j-2} - 3a_4 \varepsilon(\sigma)^2 + a_2 (T - T_c) > 0. \quad (13)$$

The effect of α in (12) is that the phase transition from Austenite to Martensite at T_c , which would occur without mean-field effects, occurs at a lower temperature $T_c - \alpha/a_2$. Therefore, if $\alpha \geq a_2 T_c$, then the phase transition can never occur. While it may be possible to engineer an SMA to remain in the “high-temperature” phase at temperatures near absolute zero, most SMAs do not exhibit this behavior in practice. We expect the mean-field constant to lie in the range $\alpha \in [0, a_2 T_c)$. In general, the mean-field constant is material-dependent and we estimate it through least-squares fits to experimental data.

3. THE DOMAIN WALL MODEL

The nonlinear equations (12) and (13) adequately describe the equilibrium response of an SMA. However, as mentioned in the previous sections, this Landau-based constitutive theory suggests that the SMA responds instantaneously when brought across a transition point, which is typically not observed in experiments [11, 19, 28]. Realistically, ferroelastics contain material inclusions and other inhomogeneities that effectively prevent a bulk specimen from transforming uniformly and instantly. Therefore, we treat the measured strain ε of an SMA as a result of crystal reorientations impeded by lattice defects. The component of the measured strain responsible for the crystallographic reorientation alone is referred to as the *anhysteretic strain*, ε_{an} [15, 22, 24]. This strain component, which we model in (12), minimizes the effective Gibbs free energy (3) for fixed temperature and stress. In this section, we quantify the effects of the material inclusions and we develop a model that incorporates (12) to predict the measured strain ε .

3.1. Characterization of Domain Wall Pinning

A *domain* consists of a homogeneous region of an ferroelastic crystal consisting a single phase with a particular deformation strain. The boundary between different domains is termed a *domain wall*, and in SMAs, domain walls represent the interfaces between regions of Austenite and Martensite phases. The movement of a domain

wall occurs when domains undergo a phase transformation. A *pinning site* characterizes some material impurity, inclusion, or inhomogeneity that effectively hinders the natural motion of domain walls. As treated in [15, 22, 24], we assume that the energy per unit volume required to move a domain wall through a pinning site is proportional to the average energy per unit volume associated with unimpeded domain wall movement. Let k represent a pinning energy density related to the maximum change in strain exhibited by an SMA. Then, as detailed in [16], the total pinning energy has the form

$$\mathbf{E}_p = k \int_V d\varepsilon, \quad (14)$$

where the integral represents the average strain over the SMA volume V . In other words, the energy per domain wall needed to move across an inclusion is proportional to the measured strain.

3.2. Balance of energy

The total work performed by an effective stress to strain a ferroelastic crystal is the elastic energy required to reconfigure the crystal lattice minus the energy needed to move material domain walls across pinning sites. Therefore, an SMA under stress has the following balance of elastic energy

$$\int_V \varepsilon d\sigma_e = \int_V \varepsilon_{an}(\sigma_e) d\sigma_e - k \int_V \left(\frac{d\varepsilon}{d\sigma_e} \right) d\sigma_e. \quad (15)$$

Differentiating (15) with respect to the effective stress yields the equation of state relation

$$\varepsilon = \varepsilon_{an}(\sigma_e) - \delta k \frac{d\varepsilon}{d\sigma_e}, \quad (16)$$

where δ ensures that the direction of the resistive pinning forces is opposite the direction of the effective stress

$$\delta = \begin{cases} +1 & \text{increasing } \sigma_e \\ -1 & \text{decreasing } \sigma_e. \end{cases}$$

Using (11) and the chain rule, (16) reduces to a nonlinear ODE in terms of total strain ε and applied stress σ

$$\frac{d\varepsilon}{d\sigma} = \frac{\varepsilon_{an}(\sigma_e) - \varepsilon(\sigma)}{\delta k + \alpha [\varepsilon_{an}(\sigma_e) - \varepsilon(\sigma)]}.$$

In summary, our model predicting strains of an SMA due to external loading is represented by solutions to the problem

$$\frac{d\varepsilon}{d\sigma} = \frac{\varepsilon_{an}(\varepsilon, \sigma) - \varepsilon}{\delta k + \alpha [\varepsilon_{an}(\varepsilon, \sigma) - \varepsilon]}, \quad \varepsilon(0) = 0, \quad (17)$$

where $\varepsilon_{an}(\varepsilon, \sigma)$ is a real value such that

$$\sum_{j=3}^m a_{2j} \varepsilon_{an}^{2j-1} - a_4 \varepsilon_{an}^3 + a_2 (T - T_c) \varepsilon_{an} = \sigma - \alpha \varepsilon(\sigma) \quad (18)$$

and

$$\sum_{j=3}^m (2j-1) a_{2j} \varepsilon_{an}^{2j-2} - 3a_4 \varepsilon_{an}^2 + a_2 (T - T_c) > 0. \quad (19)$$

In effect, the domain wall model quantifies the motion of phase boundaries across inclusions, relative to their ideal motion in the absence of inclusions. Note that in the domain wall models for ferromagnetic [15] and

ferroelectric [22] materials, “irreversible” magnetization and polarization takes the place of the strain ε in (17). These other domain wall models also define a “reversible” component. Our initial comparisons to data indicate that analogous reversible strain components for SMAs provide lower-order effects and hence can be neglected for initial material characterization.

4. MODEL VALIDATION

We compare our model to data from NiTi stress-strain experiments conducted by Shaw and Kyriakides [19], which account for strain-rate effects in establishing isothermal conditions. Shaw and Kyriakides observed that if they strained an SMA too quickly, it did not completely dissipate latent heats released during phase transformations, thereby inducing *material self-heating*. They measured changes in SMA temperatures as much as 28°C during a stress-strain cycle at a moderate strain-rate. To reduce self-heating, Shaw and Kyriakides performed a series of displacement-controlled experiments at low strain rates in an isothermal liquid bath. They show that at a strain rate of $4 \times 10^{-4} \text{ s}^{-1}$ in a water environment, SMA temperatures vary no more than 1°C. Our isothermal model is capable of predicting SMA behavior under these conditions.

Using our model with $m = 7$ for the anhysteretic relation (18), we performed a least-squares fit to identify the nine material-dependent parameters. The temperatures T and T_c are obtained from measurements. Table 1 lists the values of the parameters employed in the model. Figure 5 shows the model simulation with the experimental data. The data corresponds to tensile experiments on polycrystalline, NiTi wire of 1.07 mm diameter with at. 50.1% Ni composition. In contrast to the anhysteretic model alone, the domain wall model quantifies strains during the phase transitions and provides an accurate characterization of the experimentally measured material behavior.

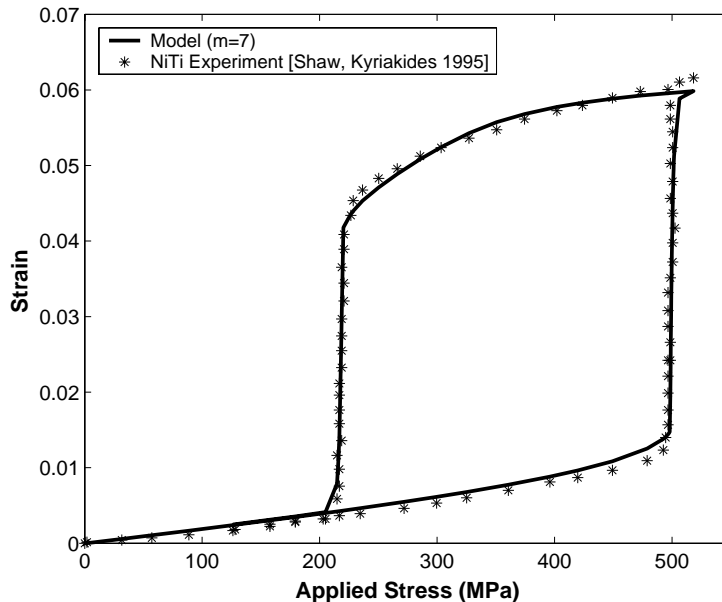


Figure 5: Experimental NiTi stress-strain data and model fit with the $m = 7$ model.

a_2	a_4	a_6	a_8	a_{10}	a_{12}
$1.13 \times 10^3 \text{ MPa/K}$	1.06×10^8	1.05×10^{11}	-5.88×10^{13}	1.94×10^{16}	-3.52×10^{18}
a_{14}	α	k	T_c	T	
2.69×10^{20}	1.40×10^{-2}	2.00 J/m^3	287 K	333.2 K	

Table 1: Parameters $a_4, a_6, a_8, a_{10}, a_{12}, a_{14}$, and α are in MPa .

5. CONCLUDING REMARKS

In this paper, we have developed a phenomenological model for pseudoelasticity in SMAs. We use the Landau theory of phase transitions to derive nonlinear stress-strain equations and we incorporate domain wall pinning to account for impeded motion of phase boundaries. The resulting isothermal model is analogous to the domain wall models developed in [15] for ferromagnetics, in [22] for ferroelectrics, and introduced in [28] for second-order ferroelastics. Altogether, our model requires $m + 2$ ($m \geq 3$ is odd) material-dependent, effective parameters that we identify through least-squares fit to data. In addition, the model employs two measured temperatures. We show that $m = 7$ provides excellent agreement with experimental data; however, as few as seven parameters total may provide sufficient accuracy for many control applications. Moreover, our model is based on a single first order, nonlinear ordinary differential equation. The simplicity of our model makes it viable for real-time implementation in model-based controllers. In particular, inverse compensator control methods have been used with ferromagnetic domain wall models. In a similar fashion, we will consider this control method with our ferroelastic model.

Currently, our model does not quantify the effects of stress rate. To accommodate SMAs in more practical operating conditions, we intend to incorporate these effects in such a way that we do not sacrifice the simplicity or accessibility of the model. In addition, while the current anhysteretic stress-strain equations (12) can approximate strain-temperature hysteresis, the shape memory effect, and latent heats of transformation [7], we intend to modify our full domain wall model to deal with dynamic temperature conditions. Incorporating anisothermal conditions will allow us to investigate the thermal actuation of thin-film SMAs for use in MEMS devices.

ACKNOWLEDGMENTS

This research was supported in part by the National Science Foundation under the grant CMS-0099764.

REFERENCES

1. S. Aizawa, T. Kakizawa and W. Higashino, "Case studies of smart materials for civil structures," *Smart Materials and Structures*, **7**(5), pp. 617-626, 1998.
2. A. Bhattacharyya and V. Stoilov, "One-dimensional sharp phase front-based continuum models of phase transformations in shape memory alloys," *Smart Structures and Materials 2000: Active Materials: Behavior and Mechanics*, pp. 524-535, 2000.
3. K. Bhattacharyya and R.V. Kohn, "Symmetry, texture and the recoverable strain of shape-memory polycrystals," *Acta Materialia*, **44**(2), pp. 529-42, 1996.
4. L.C. Brinson and M.S. Huang, "Simplifications and comparisons of shape memory alloy constitutive models," *Journal of intelligent material systems and structures*, Vol. 7, pp. 108-114, 1996.

5. M. Brokate and J. Sprekels. *Hysteresis and Phase Transitions*, Applied Mathematical Sciences Volume 121. Springer, New York, NY, 1996.
6. J. Gill, D. Chang, et. al., "Manufacturing issues of thin film NiTi microwrapper," *Sensors and Actuators A: Physical*, **93**(2), pp. 148-156, 2001.
7. F. Falk, "One-dimensional model of shape memory alloys," *Archives of Mechanics*, **35**(1), pp. 63-84, 1983.
8. F. Falk, "Pseudoelastic stress-strain curves of polycrystalline shape memory alloys calculated from single crystal data," *Int. J. Engng. Sci.*, **27**(3), pp. 277-84, 1989.
9. F. Falk, P. Konopka, "Three-dimensional Landau theory describing the martensitic phase transformation of shape-memory alloys," *J. of Physics: Condensed Matter*, **2**(1), pp. 61-77, 1990.
10. F. Falk, "Constitutive theories of shape memory alloys related to microstructure," *Proc. of the SPIE –The Int. Soc. for Optical Eng.*, Vol. 2442, pp. 2-10, 1995.
11. H. Funakubo. *Shape Memory Alloys.*, translated from the Japanese by J.B. Kennedy, Gordon and Breach Science Publishers, Amsterdam, 1987.
12. K. Gall, H. Sehitoglu and Y. Chumalakov, "NiTi experiments versus modeling: Where do we stand?" *Smart Structures and Materials 2000: Active Materials: Behavior and Mechanics, Proceedings of the SPIE*, Vol. 3992, pp. 536-547, 2000.
13. R. Gorbet, K. Morris. and D. Wang, "Passivity-based stability and control of hysteresis in smart actuators," *IEEE Transactions on Control Systems Technology*. **9**(1), pp. 5-16, 2001.
14. Y. Huo, "A mathematical model for the hysteresis in shape memory alloys," *Continuum Mechanics and Thermodynamics*, **1**(4), pp. 283-303, 1989.
15. D.C. Jiles and D.L. Atherton, "Theory of ferromagnetic hysteresis," *Journal of Magnetism and Magnetic Materials.*, **61**(1-2), pp. 48-60, 1986.
16. J.E. Massad and R.C. Smith, "An Energy Based Model for Ferroelastic Compounds," *Journal of Intelligent Material Systems and Structures*, to be submitted.
17. N. Papenfuss and S. Seelecke, "Simulation and control of SMA actuators," *Smart structures and materials 1999: Mathematics and control in smart structures, Proceedings of the SPIE*, vol 3667, pp. 586-95, 1999.
18. E. Patoor and M. Berveiller "Micromechanical modeling of the thermomechanical behavior of shape memory alloys," *Mechanics of Solids with Phase Changes*, pp. 121-188, 1997.
19. J.A. Shaw and S. Kyriakides, "Thermodynamic aspects of NiTi," *J. Mech. Phys. Solids*, **43**(8), pp. 1243-1281, 1995.
20. E.K.H. Salje. *Phase Transitions in ferroelastic and co-elastic crystals*. Cambridge University Press, 1993.
21. S. Seelecke and I. Müller, "Shape Memory Alloy Actuators in Smart Structures- Modeling and Simulation", *ASME Applied Mechanics Reviews*, submitted, 2000.
22. R.C. Smith and C.L. Hom, "Domain wall theory for ferroelectric hysteresis," *Journal of Intelligent Material Systems and Structures*, **10**(3), pp. 195-213, 1999.
23. R.C. Smith and J.E. Massad, "A Unified Methodology for Modeling Hysteresis in Ferroic Materials," *Center for Research in Scientific Computation Technical Report CRSC-TR01-10; Proceedings of the 18th ASME Biennial Conference on Mechanical Vibration and Noise*, to appear.

24. R.C. Smith and Z. Ounaies, "A domain wall model for hysteresis in piezoelectric materials," *Journal of Intelligent Material Systems and Structures*, **11**(1), pp. 62-79, 2000.
25. J.W. Tester and M. Modell. *Thermodynamics and Its Applications*, 3rd. Ed., Prentice Hall PTR, 1997.
26. P. Tolédano, M. Fejer and B. Auld, "Nonlinear elasticity in proper ferroelastics," *Physical Review B*, **27**(9), pp. 5717-5744, 1983.
27. P. Tolédano and V. Dmitriev. *Reconstructive Phase Transitions*, World Scientific, New Jersey, 1996.
28. J.A. Tuszynski, B. Mróz, et. al., "Comments on the hysteresis loop in ferroelastic LiCsSO₄," *Ferroelectrics*, **77**, pp. 111-120, 1988.
29. D. Xu, L. Wang, et. al., "Characteristics and fabrication of NiTi/Si diaphragm micropump," *Sensors and Actuators A: Physical*, **93**(1), pp. 87-92, 2001.